Ab Initio Comparison of Bonding Environments and Threshold Behavior in Ge x As 10 Se 90− x and Ge x Sb 10 Se 90− x Glass Models

ARTICLE *in* THE JOURNAL OF PHYSICAL CHEMISTRY A · MAY 2015

Impact Factor: 2.69 · DOI: 10.1021/acs.jpca.5b00039 · Source: PubMed

THE JOURNAL OF PHYSICAL CHEMISTRY A

Article

pubs.acs.org/JPCA

Ab Initio Comparison of Bonding Environments and Threshold Behavior in $Ge_xAs_{10}Se_{90-x}$ and $Ge_xSb_{10}Se_{90-x}$ Glass Models

George Opletal,*[,†,∥] Daniel W. Drumm,[†,⊥] Timothy C. Petersen,[‡] Rong P. Wang,[§] and Salvy P. Russo[†]

[†]Theoretical Chemical and Quantum Physics, School of Applied Sciences, RMIT University, 124 La Trobe Street, Melbourne, Victoria 3000, Australia

[‡]School of Physics and Astronomy, Monash University, Clayton 3800, Victoria, Australia

[§]Centre for Ultrahigh Bandwidth Devices for Optical Systems (CUDOS), Laser Physics Centre, Research School of Physics and Engineering, The Australian National University, Canberra, ACT 0200, Australia

ABSTRACT: Ab initio models of $Ge_xAs_{10}Se_{90-x}$ and $Ge_xSb_{10}Se_{90-x}$ glasses are constructed, and their bonding environments are characterized and compared against each other and to recent experimental studies of equivalent glasses at the same stoichiometry and density. A minimum in the linear refractive index is found to correlate with a maximum in the number of length-one, predominantly Se, atomic chains for both glass types. The threshold behavior difference between GeAsSe and GeSbSe is shown to be due to the appearance of As−As−Se_2 structural units beyond the MCN = 2.67 threshold in the GeAsSe glasses.

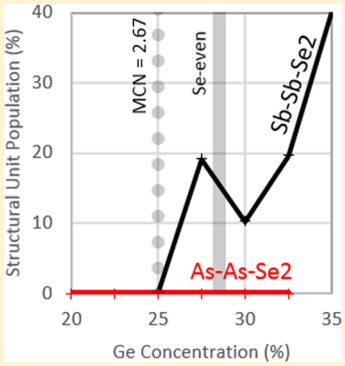

1. INTRODUCTION

Chalcogenide glasses have received substantial interest due to their optoelectronic properties and promising application as candidate materials for photonic devices.[1,2] Ternary glasses such as GeAsSe and GeSbSe, with their wide glass-formation windows and elemental tunability, are of particular interest. As such, understanding their physical properties and underlying chemical environments as functions of elemental concentrations is of fundamental importance.

The elemental concentrations can be related to the mean coordination number (MCN) via an assumption of the $8 - N$ rule, where N is the number of electrons in the valence shell of a particular element in the glass. For GeAsSe and GeSbSe glasses relevant to this work, which contain 4, 5, and 6 electrons respectively, Ge, As/Sb, and Se can ideally bond with 4, 3, and 2 nearest neighbors, a result supported by EXAFS experiments.[3] This gives an MCN of $\langle r\rangle = 4N_{Ge} + 3N_{As} + 2N_{Se}$, where N_{Ge} and N_{As} are the fractions of Ge and As/Sb atoms (for the GeSbSe system, N_{As} is replaced with N_{Sb}), and $N_{Se} = (1 - N_{Ge} - N_{As})$ is the fraction of Se atoms.

Using the MCN, constraint-counting models have predicted the existence of a number of phases within these ternary glasses. Phillips[4,5] defined the average number of constraints per atom as $n = \langle r\rangle/2 + (2\langle r\rangle - 3)$. If n is less than the number of degrees of freedom per atom (equal to three) in a three-dimensional network, then the network is defined as underconstrained or "floppy". When n is greater than 3, then it is defined as overconstraint or rigid. When it is equal to 3, it is labeled as isostatic and this occurs at $\langle r\rangle = 12/5 = 2.4$, marking the boundary between these two topological phases. A second transition was detailed by Tanaka[6,7] beyond $\langle r\rangle = 2.4$, where the average number of constraints per atom is then given by $n = \langle r\rangle/2 + (\langle r\rangle - 1)$ and a transition occurs at $\langle r\rangle = 8/3 \approx 2.67$. This transition marks a change from a rigid two-dimensional planar network to a rigid and stressed three-dimensional phase.

With ternary systems, a further complication arises in that a particular value of the MCN does not uniquely define the elemental concentrations. As such, for a particular MCN an ideal stoichiometric composition marks the chemical threshold where the number of Se atoms is sufficient to saturate all the Ge and As/Sb bonds without requiring any homonuclear bonding (labeled Se-even). In terms of the Se atoms, the concentration for this condition is given by $N_{Se\text{-}even} = \langle r\rangle/4$ with $\langle r\rangle$ ranging from 2.4 (N_{Ge}= 0 and N_{As} = 0.4) to 2.67 (N_{Ge} = 0.33 and N_{As} = 0.0), which represent the earlier discussed floppy- and rigid-phase boundaries. However, ternary glasses at a fixed MCN value can also have an excess or deficit of Se atoms. If $N_{Se} > N_{Se\text{-}even}$ (requiring more Ge atoms and less As atoms to maintain constant MCN), the glass is labeled Se-rich and contains significant Se−Se bonding. If $N_{Se} < N_{Se\text{-}even}$ (requiring less Ge atoms and more As atoms), then the glass is Se-poor and contains Ge−Ge and As−As homonuclear bonding.

Many experimentally measured quantities have extrema near these transition points. For example, when the As concentration is held constant and the MCN concentration is increased (increasing the Ge content of the glass), the densities

Received: January 3, 2015
Revised: May 10, 2015
Published: May 18, 2015

DOI: 10.1021/acs.jpca.5b00039
J. Phys. Chem. A 2015, 119, 6421−6427

Table 1. Summary of Structural Models[a]

composition	density (g/cm^3)	cell length (Å)	Ge	As or Sb	Se	8 − N MCN	se excess
$Ge_{20}As_{10}Se_{70}$	4.412	19.113	48	24	168	2.50	very rich (15)
$Ge_{22.5}As_{10}Se_{67.5}$	4.394	19.126	54	24	162	2.55	rich (7.5)
$Ge_{25}As_{10}Se_{65}$	4.363	19.157	60	24	156	2.60	even (0)
$Ge_{27.5}As_{10}Se_{62.5}$	4.345	19.171	66	24	150	2.65	poor (−7.5)
$Ge_{30}As_{10}Se_{60}$	4.348	19.153	72	24	144	2.70	very poor (−15)
$Ge_{32.5}As_{10}Se_{57.5}$	4.370	19.108	78	24	138	2.75	very poor (−22.5)
$Ge_{35}As_{10}Se_{55}$	4.400	19.051	84	24	132	2.80	very poor (−30)
$Ge_{10}Sb_{10}Se_{80}$	4.613	19.253	24	24	192	2.30	very rich (45)
$Ge_{15}Sb_{10}Se_{75}$	4.615	19.226	36	24	180	2.40	very rich (30)
$Ge_{20}Sb_{10}Se_{70}$	4.601	19.221	48	24	168	2.50	very rich (15)
$Ge_{22.5}Sb_{10}Se_{67.5}$	4.586	19.229	54	24	162	2.55	rich (7.5)
$Ge_{25}Sb_{10}Se_{65}$	4.541	19.280	60	24	156	2.60	even (0)
$Ge_{27.5}Sb_{10}Se_{62.5}$	4.570	19.226	66	24	150	2.65	poor (−7.5)
$Ge_{30}Sb_{10}Se_{60}$	4.604	19.167	72	24	144	2.70	very poor (−15)
$Ge_{32.5}Sb_{10}Se_{57.5}$	4.654	19.085	78	24	138	2.75	very poor (−22.5)

[a]The 8 − N MCN is the theoretical MCN value, under the assumption of Ge, As, or Sb and Se having 4, 3, and 2 bonds, respectively. The Se excess shows the deviation from an ideal 8 − N stoichiometry. This ideal value is given by $2N_{Ge} + 1.5N_{As}$.

of GeAsSe glasses have been observed to have a maximum at $\langle r \rangle = 2.4$ and a minimum at $\langle r \rangle = 2.67$ across a range of fixed As-composition glasses.[8] A similar observation is seen in regard to the linear refractive index where, for GeAsSe glasses, a minimum is found around $\langle r \rangle = 2.67$ across a range of constant-As compositions,[9] which placed these glasses in the Se-poor regime.

On the contrary, similar experiments with GeSbSe glasses (holding the Sb concentration constant and varying the Ge concentration and MCN), shows that this MCN threshold behavior around 2.4 and 2.67 is not universal. Instead, for GeSbSe, the refractive index minimum does not occur at some fixed MCN value but occurs only for Se even glasses.[10] The GeAsSe/GeSbSe refractive index comparison highlights a complication due to the chemical composition not accounted for in the constraint-counting models detailed earlier. Within GeSbSe glasses, this chemical effect has been previously explained by a "demixing" of the network into separate phases of Ge−Se_4 and Ge−Sb_3 structural units on the nano- or microscale[10,11] above the Se-even stoichiometric threshold. In this work, we develop atomistic ab initio models of $Ge_xAs_{10}Se_{90-x}$ and $Ge_xSb_{10}Se_{90-x}$ glasses to compare and characterize their chemical environments across these transition boundaries with the aim of elucidating the origins of different behavior. We use the same stoichiometric compositions and densities from previous experimental studies[8−10,12] to be able to directly relate these models to experimental samples.

2. METHODOLOGY

Seven GeAsSe and eight GeSbSe models were prepared with the fraction of As and Sb atoms at 10%, mimicking the experimental density and stoichiometry of previous experimental studies.[8−10,12] Initial configurations were generated via the reverse Monte Carlo (RMC) method[13] (using the hybrid reverse Monte Carlo code[14]) before being temperature quenched via ab initio MD simulations using the Vienna ab initio simulation package (VASP).[15] A similar procedure has been used in previous models for GeAsSe.[16−18] In particular, it was shown[18] that the lowest energy models resulted from a combination of RMC initial structures followed by subsequent MD quench simulations. A summary of the models is shown in Table 1.

The 240-atom systems were initially generated using the RMC methodology over 50 million attempted steps to reduce the amount of sampling required in configuration space.[18] For all systems, a number of constraints were used:

(i) Ge, As/Sb, and Se have 4, 3, and 2 nearest neighbors, respectively, as supported by extended X-ray absorption fine structure (EXAFS) studies.[3,19]
(ii) There is minimal homonuclear bonding, ensuring maximal values of Ge−Se and As−Se (or Sb−Se) bonds, supported by EXAFS studies—particularly for Se-even glasses.[19]
(iii) There is no three-membered ring formation; these can arise from under-constrained RMC simulations.[20]
(iv) Fitting to a bond-angle distribution and radial distribution function derived from previous ab initio models.[17]

These models were then used as initial starting structures for ab initio MD simulations using VASP and quenched at a constant density to room temperature. In previous work on similar systems,[18] it was shown that short ab initio simulations quenched from a melt have a tendency to "freeze-in" unphysical structural artifacts from the melt that do not exist at room temperature. This is minimized by not using excessively high starting temperatures in the liquid state and ensuring a sufficiently long simulation time for the temperature quench. A common starting temperature of 1000 K was used for all the initial RMC structures. This value was chosen by looking at the experimental glass transition temperatures,[8] which increase from 481 K for $Ge_{20}As_{10}Se_{70}$ to 646 K for $Ge_{35}As_{10}Se_{55}$ and also increase from 394.5 K for $Ge_{10}Sb_{10}Se_{80}$ to 558 K for $Ge_{32.5}Sb_{10}Se_{57.5}$. Previous GeAsSe studies[16,17] have used 2000 K for 20 ps with a linear quench to 300 K over 30 ps and equilibration at 300 K for 10 ps for their quench procedure. More recently,[18] this was improved on by starting at 1000 K and quenching over 48 ps to room temperature. In this work, we equilibrated at 1000 K for 60 ps in the liquid state and quenched linearly to 300 K over 120 ps before equilibrating at 300 K for a further 60 ps. The mean square displacement was calculated and checked toward the end of the 1000 K equilibration phase to ensure that the initial structures had melted.

DOI: 10.1021/acs.jpca.5b00039
J. Phys. Chem. A 2015, 119, 6421−6427

The constant number of atoms, volume, and temperature (*NVT*) MD simulations used a Nosé−Hoover thermostat and were performed under the generalized gradient approximation (GGA) using a Perdew−Wang (PW91) exchange−correlation functional[21] and ultrasoft pseudopotentials.[22,23] A 2 × 2 × 2 Monkhorst−Pack *k*-point sampling scheme[24] around the Γ point was used, a plane-wave cutoff of 155.2 eV with a Methfessel−Paxton smearing[25] of order 2 and a time step of 3 fs.

The coordination numbers, bond type, and chain length populations were then obtained by averaging over the final 1000 configurations or 3 ps at 300 K. Nearest neighbors for the GeAsSe systems were defined by cutoff distances of 3.0 Å for Ge−Se bonds and 2.85 Å for all other bonds. For the GeSbSe systems, the cutoffs defining the nearest neighbors were 3.0 Å for Ge−Se and Sb−Se bonds and 2.7 Å for the rest. These values were chosen on the basis of the separation minimum between the first and second peaks of the partial $g(r)$ curves from preliminary RMC simulations. Some element pairs (such as Ge−Se and Sb−Se) did not have a zero value between the first and second peaks and thus required specific definition. The values chosen were adjusted as to not introduce significant 4-fold nearest neighbors for As/Sb and 5-fold nearest-neighbor populations for Ge atoms.

3. RESULTS AND DISCUSSION

The constraint-counting models assume a four-, three-, and 2-fold coordination for Ge, As/Sb, and Se atoms, as supported by EXAFS studies[3,19] over a wide range of compositions with an uncertainty of ±0.1. Figure 1 shows the average elemental- and mean-coordination numbers for all models in this work, illustrating that the ab initio simulations deviate away from this ideal situation. With increasing Ge concentration, we see increasing overcoordination of Se and As/Sb atoms (with Sb atoms having significantly higher overcoordination than As atoms) and an undercoordination of Ge atoms. Overall, the MCN roughly follows the trend expected by the 8 − *N* rule although the discrepancy tends to increase with increasing MCN. The overcoordination of Sb compared to As may be significant. The replacement of As by Sb in Ge−As(Sb)−Se glasses can induce a significant departure from the idealized constraint counting models, which tend to have their properties predominantly determined by the MCN alone. This chemical effect of the element Sb has been recently observed in measurements of the elastic moduli in GeAsSe and GeSbSe glasses.[8] A possible origin of this effect in GeSbSe glasses could be due to the increase of the p-orbital contribution to the chemical bond, which may lead to higher Sb coordination numbers. Looking at the model MCN of $Ge_{25}Sb_{10}Se_{65}$, as opposed to the 8 − *N* rule, which assumes four, three, and two bonds for Ge, Sb, and Se, respectively, for an expected overall MCN of 2.6, we find instead that this Se-even model has an MCN of 2.67 due to its elemental coordination numbers (ECNs) of 3.67, 3.14, and 2.22 for Ge, Sb, and Se atoms, respectively. With the EXAFS-derived ECNs of Sen et al.[3] and Wang et al.[19] having an uncertainty of ±0.1, a small amount of overcoordination (less than observed in our simulations) may be consistent with experiments. The difficulty of achieving ideal ECNs when quenching from melt in ab initio simulations, in particular for germanium, has been highlighted in our previous work[16−18] and in the $Ge_{20}As_{40}Se_{40}$ model of Cai et al.[26]

The bond type evolution as a function of Ge concentration is shown in Figure 2. Particular care needs to be taken when the As/Sb results are interpreted, due to the low numbers of atoms of these elements in the models.

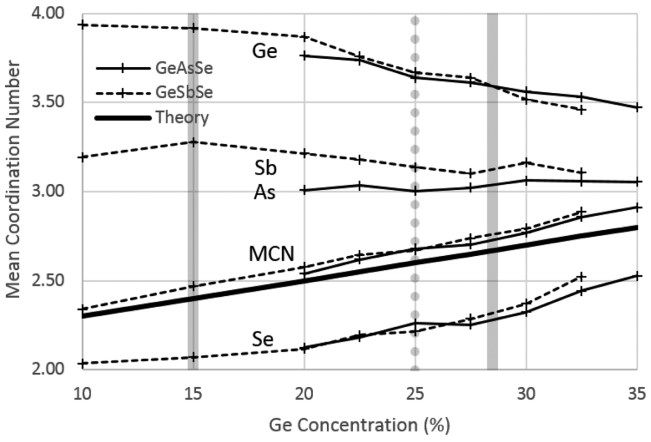

Figure 1. Mean coordination numbers for the overall system and the individual elements within the GeAsSe and GeSbSe systems. The black line is the expected overall MCN if Ge, As/Sb, and Se, respectively, have 4-, 3-, and 2-fold coordination. The thick vertical lines at 15% and 28.5% Ge concentrations are the transition lines of MCN = 2.4 and 2.67, and the 25% dotted line is the Se-even stoichiometry line.

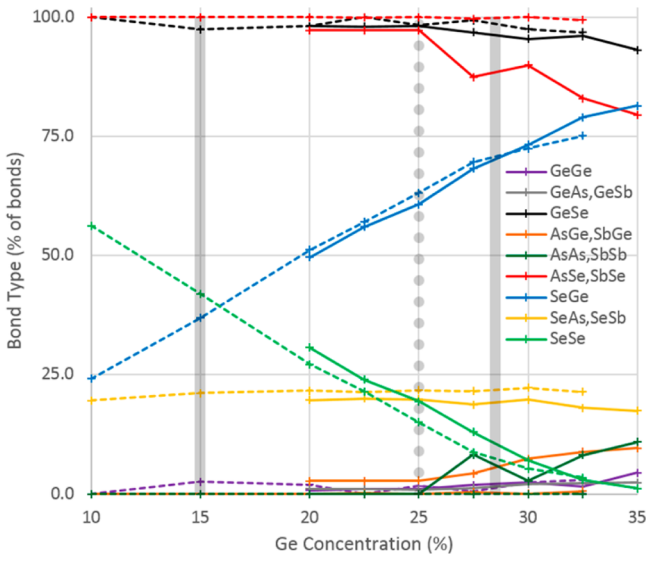

Figure 2. Bond-type percentage calculated for each element in each system. For each element, the three bond types sum to 100%. For example, SeGe + SeAs + SeSe = 100%. The dashed line represents the GeSbSe system, and the solid line represents the GeAsSe system. The thick vertical lines at 15% and 28.5% Ge concentrations are the transition lines of MCN = 2.4 and 2.67, and the 25% dotted line is the Se-even stoichiometric line.

At low Ge concentration (and low MCN), there is minimal As−As homonuclear bonding. With increasing MCN, the GeAsSe glasses show an abrupt increase in As−As bonding after the Se-even stoichiometric transition at MCN = 2.60, mostly at the cost of As−Se bonds. This is supported by X-ray photoelectron spectrum (XPS) measurements showing As−As homonuclear bonds dominating Ge−Ge bonds.[27] GeSbSe shows a smaller increase in homonuclear bonding, although in this case Ge−Ge bonds dominate Sb−Sb bonding (also supported by Raman spectroscopy[10]). The constant population

DOI: 10.1021/acs.jpca.5b00039
J. Phys. Chem. A 2015, 119, 6421−6427

of Se−As and Se−Sb bonds across a wide range of Ge concentrations has also been experimentally detected[10] along with the decreasing Se−Se bonding, which was seen in previous modeling work[16] and in Raman studies.[10] According to constraint-counting models for Se-even stoichiometry, enough Se bonds exist to saturate all the Ge and As/Sb atoms, which should theoretically result in no homonuclear bonding. These models show (along with previous models of GeAsSe glasses[16,17]) that homonuclear bonding is found even in Se-rich systems. Interestingly, recent analysis of Raman scattering and XPS experiments of GeAsSe Se-even glasses also found significant homonuclear bonding and concluded that it may be an intrinsic structural characteristic of these glasses.[28]

The population of first-nearest-neighbor structural units is shown for Ge and As/Sb in Figure 3 and Se in Figure 4. All

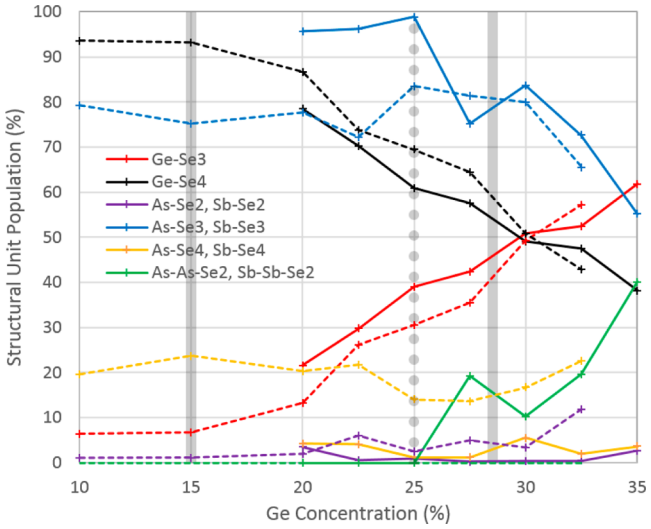

Figure 3. Dominant first-nearest-neighbor structural units for Ge and As/Sb central atoms. The dashed line represents the GeSbSe system, and the solid line represents the GeAsSe system. The thick vertical lines at 15% and 28.5% Ge concentrations are the transition lines of MCN = 2.4 and 2.67, and the 25% dotted line is the Se-even stoichiometric line.

systems contain significant undercoordinated $Ge−Se_3$ populations that increase with increasing Ge concentration. Although not shown, at higher-Ge concentrations, $Ge−Ge−Se_3$ and $Ge−Ge−Se_2$ units begin to appear in small numbers.

For the GeAsSe system some $As−Se_3$ units are replaced by $As−As−Se_2$ units after the Se-even stoichometric transition, which is consistent with the rise of homonuclear bonding in Figure 2. The rise of the $As−As−Se_2$ structural units was also seen in XPS studies with increasing Ge and As concentration.[27] The GeSbSe system does not show this behavior; there are no equivalent $Sb−Sb−Se_2$ units, and this represents a primary difference in the structural trends between these two glass compositions. The overcoordination of Sb in the GeSbSe system is due mostly to a significant population of 4-fold $Sb−Se_4$ units, whereas in the GeAsSe systems where As coordination was near-3-fold, there were minimal $As−Se_4$ overcoordinated units.

The Se structural environments show similar trends for both system types. At low Ge concentrations, the GeSbSe models are dominated by $Se−Se_2$, Ge−Se−Se, and Sb−Se−Se units. With increasing Ge concentration, we see a rise in overcoordinated

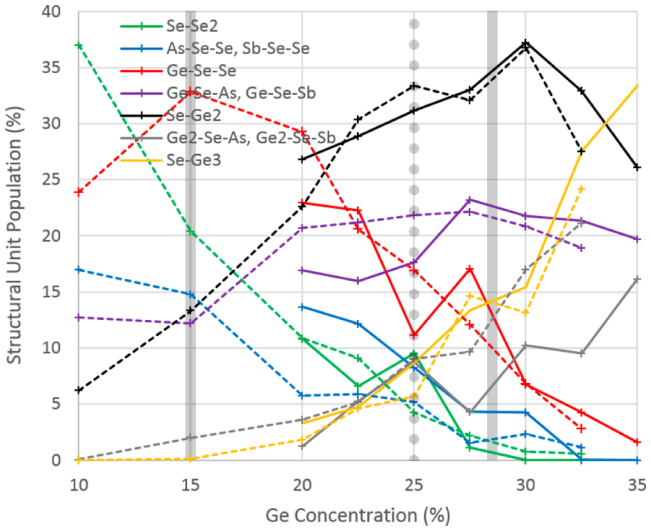

Figure 4. Dominant first-nearest-neighbor structural units for Se central atoms. The dashed line represents the GeSbSe system, and the solid line represents the GeAsSe system. The thick vertical lines at 15% and 28.5% Ge concentrations are the transition lines of MCN = 2.4 and 2.67, and the 25% dotted line is the Se-even stoichiometric line.

units in the form of $Se−Ge_3$ and $Ge_2−Se−As/Ge_2−Se−Sb$, accounting for the increase in Se coordination above 2-fold.

The decrease in $Se−Se_2$ as a function of Ge concentration is further investigated by looking at the population of 2-fold-coordinated atom-chain lengths. Code was written to calculate the population of atomic chains containing only 2-fold coordinated atoms. A single coordination-two atom with no coordination-two neighbors has a chain length of one. If two atoms each having 2-fold coordination are adjacent but surrounded by higher-coordinated atoms, the length is two, etc. These chains are almost entirely composed of Se atoms, and model diagrams of the chains are shown in Figure 5.

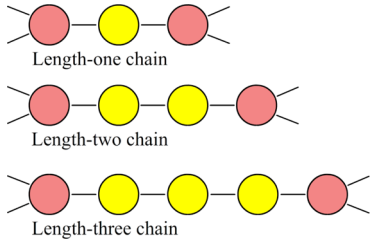

Figure 5. Illustration of the Se−Se chain length models. Each chain is terminated by atoms of coordination number 3 or higher, which are almost always Ge or As/Sb atoms.

The number of length-one chains as a function of Ge concentration is plotted in Figure 6 along with the experimentally measured linear refractive index measured at 1.55 μm.[9,10] We observe that the refractive index minima for the models occur approximately at the maximal population of length-one segments.

In GeAsSe glasses, when the Ge concentration is varied while the As concentration is held constant (analogous to this study), the refractive index minimum has been shown to be correlated with the sample density minimum occurring at a constant MCN value around the 2.67 transition across a range of As concentrations.[9] However, for GeSbSe systems, though the sample density minima occur around MCN = 2.6, the refractive

DOI: 10.1021/acs.jpca.5b00039
J. Phys. Chem. A 2015, 119, 6421−6427

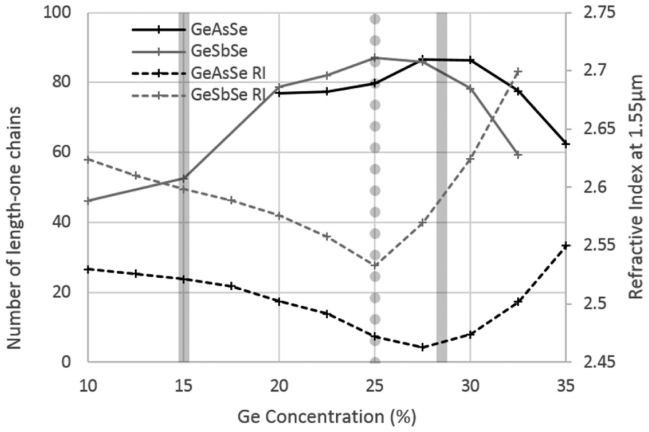

Figure 6. Number of length-one 2-fold chains for both the GeAsSe and GeSbSe systems (solid lines). Experimentally measured refractive index (RI) at 1.55 μm for both systems (dashed lines). The thick vertical lines at 15% and 28.5% Ge concentrations are the transition lines of MCN = 2.4 and 2.67, and the 25% dotted line is the Se-even stoichiometric line.

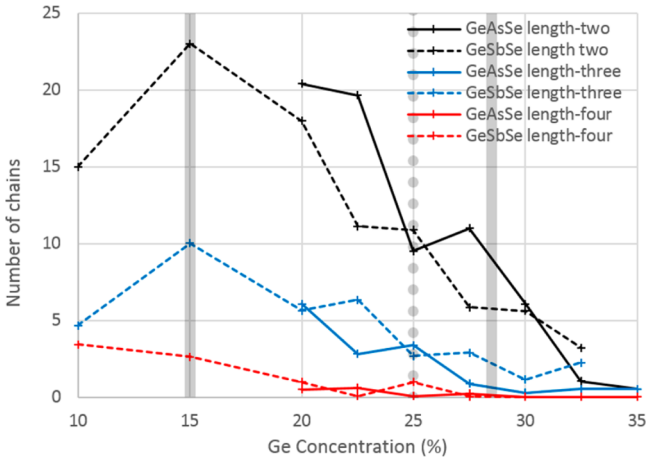

Figure 7. Number of chains of length two, three, or four for both the GeAsSe and GeSbSe systems. The thick vertical lines at 15% and 28.5% Ge concentrations are the transition lines of MCN = 2.4 and 2.67, and the 25% dotted line is the Se-even stoichiometric line.

index minima are instead correlated with Se-even stoichiometric compositions. Thus, the minima occur at MCN = 2.6 for 10% Sb concentration ($Ge_{25}Sb_{10}Ge_{65}$) and MCN = 2.53 for the 20% Sb concentration ($Ge_{16.67}Sb_{20}Se_{63.33}$). This dependence on GeSbSe was shown to be structurally correlated with a minimum in homonuclear bonding (a minimum which included Se−Se bonds) in a recent Raman spectroscopic study.[10] A network that has minimal amounts of Se−Se bonding and a minimal amount of Ge−Ge and Sb−Sb bonding is consistent with a network of Ge and Sb atoms interconnected with length-one Se chains and is thus consistent with our finding where the maximum population of length-one Se chains occurs in $Ge_{25}Sb_{10}Se_{65}$.

Interestingly, in the GeAsSe case, the maximum in the length-one chain population occurs around the MCN = 2.67 transition (the $Ge_{27.5}As_{10}Ge_{62.5}$ model), which is not a stoichiometric Se-even glass but sits in the Se-poor region. This can be explained by the rise in As−As−Se_2 structural units at the cost of As−Se_3 units, as seen in Figure 3, and the related rise in As−As homonuclear bonds in Figure 2, which increases abruptly at the MCN = 2.67 transition. Thus, at this transition, the usual three length-one Se chains found in As−Se_3 units begin to disappear as they are replaced by As−As−Se_2 which typically contain only two chains. This marks an important difference from the GeSbSe system, which does not have a similar appearance in Sb−Sb−Se_2 units and thus no corresponding rise in homonuclear bonding at the MCN = 2.67 transition.

Looking at the longer chains in Figure 7, the picture that emerges is that these longer Se chains decrease with increasing Ge concentration (with a possible maximum around the MCN = 2.4 transition in some of the shorter chains), transforming into networks where Ge and As/Sb atoms are interconnected by single-Se links correlating with a minimum in the refractive index for MCN near 2.67. A further increases in Ge concentration replaces some of these links with Ge and As/Sb homonuclear bonding.

This picture is supported by Raman spectroscopy[29] of $Ge_xSb_{10}Se_{(90-x)}$ glasses, which show a peak shift from 250 to 260 cm^{-1} as one moves to from low Ge concentrations to high, previously interpreted as a shortening of Se chains. The 260 cm^{-1} peak disappears at $x = 25$, suggesting the disappearance of these Se chains. Our GeSbSe models show a disappearance of Se chains of length four and above around $x = 25$ but still contain small populations of smaller chains containing three or two atoms. On the contrary, Se−Se bonding is experimentally seen at all compositions; even in Se-poor glasses,[30] which suggests that length two Se chains should exist beyond $x = 25$.

The structures containing the highest and lowest Ge concentrations for GeAsSe and GeSbSe are shown in Figures 8 and 9, respectively. Se chains of length two and above are highlighted in a yellow overlay whereas Ge−Se_4 tetrahedra are shown in a red polyhedral transparency. It has been theorized that for GeSbSe systems above the Se-even threshold, the network can phase separate into demixed structural units of Ge−Se_4 and Sb−Se_3 units on the nano- or microscale.[10,12] Boolchand et al.[31] suggest that, although this readily occurs in binary glasses, the effect is suppressed by chemical disorder in ternary glasses. Although our models are small, over their length scale, no such demixing was observed.

4. CONCLUSION

Ab initio models of $Ge_xAs_{10}Se_{90-x}$ and $Ge_xSb_{10}Se_{90-x}$ glasses were constructed, their bonding environments characterized and compared against experiments. It was found that the minimum in the linear refractive index for both systems coincided with a maximum in the number of length-one 2-fold chains in the network. For the GeSbSe system, this corresponds to the Se-even stoichiometry and is consistent with previous findings that correlate this also to a minimum in homonuclear bonding.[10] For the GeAsSe system, the minimum in the refractive index and the maximum population of length-one 2-fold chains occurs instead at the MCN = 2.67 transition. This occurs due to the unique appearance of As−As−Se_2 units at the cost of As−Se_3 units, resulting in an increase to homonuclear bonding beyond the transition. The equivalent effect with Sb−Sb−Se_2 units in the GeSbSe system is not observed. If this behavior also occurs at higher As concentrations when moving beyond the MCN = 2.67 transition, it could provide an alternative explanation for the different transition behavior of these two ternary glasses. No phase separation was observed in any of the systems at the length scale of these simulations.

DOI: 10.1021/acs.jpca.5b00039
J. Phys. Chem. A 2015, 119, 6421−6427

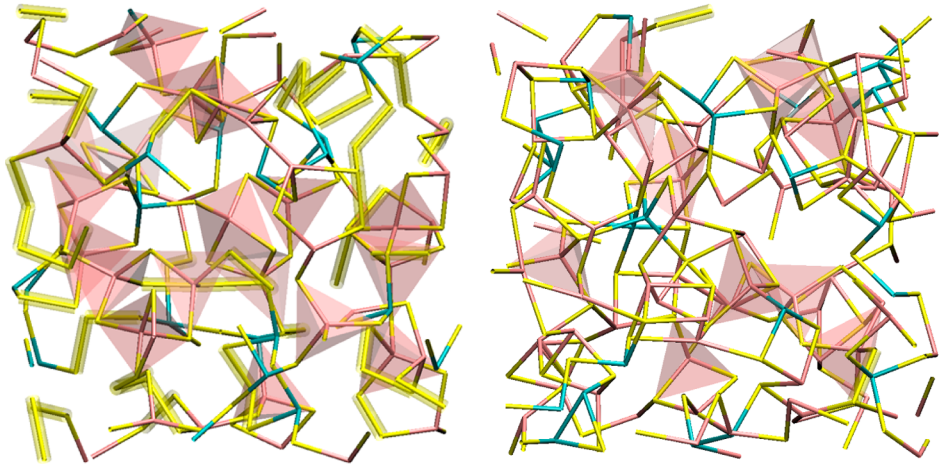

Figure 8. $Ge_{20}As_{10}Se_{70}$ (left) and $Ge_{35}As_{10}Se_{55}$ (right) final configurations with Ge, As, and Se in red, blue, and yellow, respectively. Red transparent polyhedral are centered upon Ge atoms with 4-fold coordination. Se−Se bonding is illustrated by yellow highlighting, which includes Se atom chains of length two and above. Se chains of length one (having two neighbors) are shown without highlighting along with overcoordinated lone Se atoms.

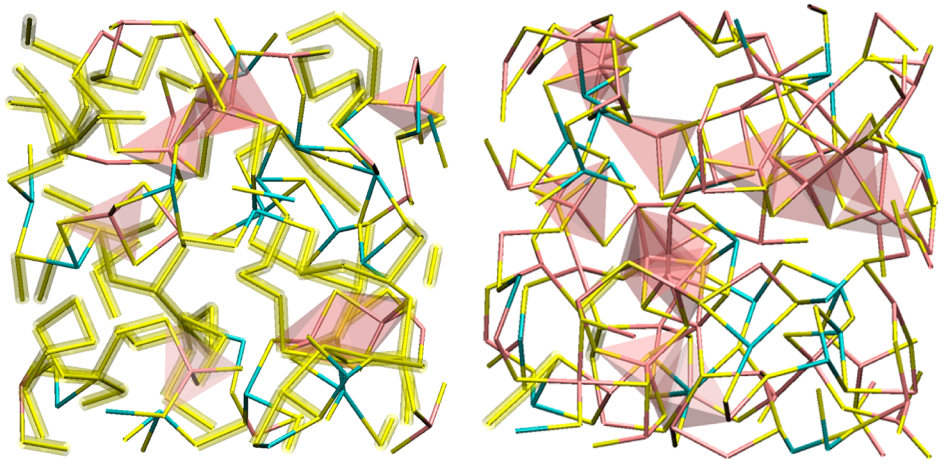

Figure 9. $Ge_{10}Sb_{10}Se_{80}$ (left) and $Ge_{32.5}Sb_{10}Se_{57.5}$ (right) final configurations with Ge, As, and Se, in red, blue, and yellow, respectively. Red transparent polyhedra are centered upon Ge atoms with 4-fold coordination. Se−Se bonding is illustrated by yellow highlighting, which includes Se atom chains of length two and above. Se chains of length one (having two neighbors) are shown without highlighting along with overcoordinated lone Se atoms.

AUTHOR INFORMATION

Corresponding Author

*G. Opletal. E-mail: george.opletal@rmit.edu.au.

Present Addresses

[‖]Theoretical Chemical and Quantum Physics, School of Applied Sciences, RMIT University, 124 La Trobe Street, Melbourne, Victoria 3000, Australia.

[⊥]Australian Resesarch Council Centre of Excellence for Nanoscale BioPhotonics, School of Applied Sciences, RMIT University, Melbourne, Victoria 3000, Australia.

Notes

The authors declare no competing financial interest.

ACKNOWLEDGMENTS

We are grateful for funding support from the Australian Research Council (ARC) Centre of Excellence for Ultrahigh Bandwidth Devices for Optical Systems (CUDOS) and the ARC discovery project DP110102753. In addition, we are thankful to the National Computational Infrastructure National Facility (NCI-NF) for the computational resources required for this study.

REFERENCES

(1) Hisakuni, H.; Tanaka, K. Optical Microfabrication of Chalcogenide Glasses. *Science* **1995**, *270*, 974−975.

(2) Saitoh, A.; Tanaka, K. Self-Developing Aspherical Chalcogenide-Glass Microlenses for Semiconductor Lasers. *Appl. Phys. Lett.* **2003**, *83*, 1725−1727.

(3) Sen, S.; Aitken, B. G. Atomic Structure and Chemical Order in Ge-As Selenide and Sulfoselenide Glasses: An X-ray Absorption Fine Structure Spectroscopic Study. *Phys. Rev. B: Condens. Matter Mater. Phys.* **2002**, *66*, 134204.

(4) Phillips, J. C. Topology of Covalent Non-Crystalline Solids I: Short-Range Order in Chalcogenide Alloys. *J. Non-Cryst. Solids* **1979**, *34*, 153−181.

(5) Thorpe, M. F. Continuous Deformations in Random Networks. *J. Non-Cryst. Solids* **1983**, *57*, 355−370.

(6) Tanaka, K. Layer Structures in Chalcogenide Glasses. *J. Non-Cryst. Solids* **1988**, *103*, 149−150.

(7) Tanaka, K. Structural Phase Transitions in Chalcogenide Glasses. *Phys. Rev. B: Condens. Matter Mater. Phys.* **1989**, *39*, 1270−1279.

(8) Wang, T.; Wei, W. H.; Shen, X.; Wang, R. P.; Jackson, I.; Luther-Davies, B. Elastic Transition Thresholds in Ge-As(Sb)-Se Glasses. *J. Phys. D: Appl. Phys.* **2013**, *46*, 165302.

DOI: 10.1021/acs.jpca.5b00039
J. Phys. Chem. A 2015, 119, 6421−6427

(9) Wang, R. P.; Luther-Davies, B. *Amorphous Chalcogenides: Advances and Applications*; Stanford Publishing: Singapore, 2014; pp 97−141.
(10) Wei, W. H.; Wang, R. P.; Shen, X.; Fang, L.; Luther-Davies, B. Correlations Between Structural and Physical Properties in Ge-Sb-Se Glasses. *J. Phys. Chem. C* **2013**, *117*, 16571−16576.
(11) Boolchand, P.; Georgiev, D. G.; Qu, T.; Wang, F.; Cai, L. C.; Chakravarty, S. Nanoscale Phase Separation Effects near r=2.4 and 2.67, and Rigidity Transitions in Chalcogenide Glasses. *C. R. Chim.* **2002**, *5*, 713−724.
(12) Wei; Wei, W. H.; Fang, L.; Shen, X.; Wang, R. P. Transition Threshold in $Ge_xSb_{10}Se_{90-x}$ Glasses. *J. Appl. Phys.* **2014**, *115*, 113510.
(13) McGreevy, R. L. Reverse Monte Carlo Modelling. *J. Phys.: Condens. Matter* **2001**, *13*, 877−913.
(14) Opletal, G.; Petersen, T. C.; Russo, S. P. HRMC_2.1: Hybrid Reverse Monte Carlo with Silicon, Germanium and Silicon Carbide Potentials. *Comput. Phys. Commun.* **2014**, *185*, 1854−1855.
(15) Kress, G.; Furthmüller, J. Efficiency of Ab-Initio Total Energy Calculations for Metals and Semiconductors Using a Plane-Wave Basis Set. *Comput. Mater. Sci.* **1996**, *6*, 15−50.
(16) Opletal, G.; Wang, R. P.; Russo, S. P. Bonding Trends Within Ternary Isocoordinate Chalcogenide Glasses $Ge_xAs_ySe_{(1-x-y)}$. *Phys. Chem. Chem. Phys.* **2013**, *15*, 4582−4588.
(17) Opletal, G.; Wang, R. P.; Russo, S. P. Investigation of Bonding Within Ab-Initio Models of GeAsSe Glasses. *Chem. Phys. Lett.* **2013**, *575*, 97−100.
(18) Opletal, G.; Drumm, D. W.; Wang, R. P.; Russo, S. P. Structural Modelling of $Ge_{6.25}As_{32.5}Se_{61.25}$ Using a Combination of Reverse Monte Carlo and Ab Initio Molecular Dynamics. *J. Phys. Chem. A* **2014**, *118*, 4790−4796.
(19) Wang, T.; Wang, R. P.; Luther-Davies, B. EXAFS Study of the Local Order in Ge-As-Se Glasses. *Phys. Procedia* **2013**, *48*, 89−95.
(20) Opletal, G.; Petersen, T. C.; O'Malley, B.; Snook, I.; McCulloch, D. G.; Marks, N.; Yarovsky, I. Hybrid Approach for Generating Realistic Amorphous Carbon Structures Using Metropolis and Reverse Monte Carlo. *Mol. Simul.* **2002**, *28*, 927−938.
(21) Perdew, J. P.; Wang, Y. Accurate and Simple Analytic Representation of the Electron-Gas Correlation Energy. *Phys. Rev. B: Condens. Matter Mater. Phys.* **1992**, *45*, 13244−13249.
(22) Vanderbilt, D. Soft Self-Consistent Pseudopotentials in a Generalized Eigenvalue Formalism. *Phys. Rev. B: Condens. Matter Mater. Phys.* **1990**, *41*, 7892−7895.
(23) Kresse, G.; Hafner, J. Norm-Conserving and Ultrasoft Pseudopotentials for First-Row and Transition Elements. *J. Phys.: Condens. Matter* **1994**, *6*, 8245−8257.
(24) Monkhorst, H. J.; Pack, J. D. Special Points for Brillouin-Zone Integrations. *Phys. Rev. B* **1976**, *13*, 5188−5192.
(25) Methfessel, M.; Paxton, A. T. High-Precision Sampling for Brillouin-Zone Integration in Metals. *Phys. Rev. B: Condens. Matter Mater. Phys.* **1989**, *40*, 3616−3621.
(26) Cai, B.; Zhang, X.; Drabold, D. A. Building Block Modelling Technique: Application to Ternary Chalcogenide Glasses g-$Ge_2As_4Se_4$ and g-$AsGe_{0.8}Se_{0.8}$. *Phys. Rev. B: Condens. Matter Mater. Phys.* **2011**, *83*, 092202.
(27) Xu, S. W.; Wang, R. P.; Luther-Davies, B.; Kovalskiy, A.; Miller, A. C.; Jain, H. Chemical Order in $Ge_xAs_ySe_{1-x-y}$ Glasses Probed by Higher Resolution X-ray Photoelectron Spectroscopy. *J. Appl. Phys.* **2014**, *115*, 083518.
(28) Xu, S.; Wang, R.; Yang, Z.; Wang, L.; Luther-Davies, B. Evidence of Homopolar Bonds in Chemically Stoichiometric $Ge_xAs_ySe_{1-x-y}$ Glasses. *Appl. Phys. Express* **2015**, *8*, 015504.
(29) Gan, Y.; Wang, L.; Su, X.; Xu, S.; Shen, X.; Wang, R. P. Thermal Conductivity of $Ge_xSb(As)_ySe_{100-x-y}$ Glasses Measured by Raman Scattering Spectra. *J. Raman Spectrosc.* **2014**, *45*, 377−382.
(30) Golovchak, R.; Shpotyuk, O.; Iovu, M.; Kovalskiy, A.; Jain, H. Topology and Chemical Order in $As_xGe_xSe_{1-2x}$ Glasses: A High-Resolution X-ray Photoelectron Spectroscopy Study. *J. Non-Cryst. Solids* **2011**, *357*, 3454−3460.
(31) Boolchand, P.; Chen, P.; Vempati, U. Intermediate Phases, Structural Variance and Network Demixing in Chalcogenides: The Unusual Case of Group V Sulfides. *J. Non-Cryst. Solids* **2009**, *355*, 1773−1785.

DOI: 10.1021/acs.jpca.5b00039
J. Phys. Chem. A 2015, 119, 6421−6427